

Article

Multi-Channeled Polymeric Microsystem for Studying the Impact of Surface Topography on Cell Adhesion and Motility

Andres Diaz Lantada ^{1,*}, Hernán Alarcón Iniesta ² and Josefa Predestinación García-Ruíz ²

Received: 16 July 2015; Accepted: 11 November 2015; Published: 23 November 2015

Academic Editors: Esmail Jabbari and Jianxun Ding

¹ Product Development Lab, Mechanical Engineering Department, Universidad Politecnica de Madrid, c/ Jose Gutierrez Abascal 2, Madrid 28006, Spain

² Molecular Biology Department, Universidad Autónoma de Madrid, Cantoblanco-Madrid 28049, Spain; hernan.alarcon@estudiante.uam.es (H.A.I.); josefap.garcia@uam.es (J.P.G.-R.)

* Correspondence: adiaz@etsii.upm.es; Tel.: +34-91-336-3120; Fax: +34-91-336-3118

Abstract: This paper presents the complete development and experimental validation of a microsystem designed to systematically assess the impact of surface topography on cell adhesion and dynamics. The microsystem includes two pools for culturing cells and for including chemicals. These pools are connected by several channels that have different microtextures, along which the cells crawl from one well to another. The impact of channel surface topography on cell performance, as well as the influence of other relevant factors, can therefore be assessed. The microsystem stands out for its being able to precisely define the surface topographies from the design stage and also has the advantage of including the different textures under study in a single device. Validation has been carried out by culturing human mesenchymal stem cells (hMSCs) on the microsystem pre-treated with a coating of hMSC conditioned medium (CM) produced by these cells. The impact of surface topography on cell adhesion, motility, and velocity has been quantified, and the relevance of using a coating of hMSC-CM for these kinds of studies has been analyzed. Main results, current challenges, and future proposals based on the use of the proposed microsystem as an experimental resource for studying cell mechanobiology are also presented.

Keywords: biomedical microdevices; surface topography; fractal geometry; biomimetic devices; cell culture; cell dynamics; tissue engineering

1. Introduction

Material surface topography has an extraordinary influence on several relevant properties linked to final material (and device) performance. These properties include friction coefficient [1], wear resistance [2], self-cleaning ability [3], biocompatibility [4], optical response [5], aesthetics, and other properties linked to our senses [6]. As a consequence, topography is a fundamental property for material selection in engineering, especially in areas linked to micro and nanosystem development and to biomedical engineering, where these effects are even more relevant.

In the field of tissue engineering and regenerative medicine, surface topography plays a determinant role in several strategies, both *in vitro* and *in vivo*, as it affects the adhesion of cells to materials, substrates, and biodevices; not just for *in vitro* studies, but also for implantation and living tissue repair. It also influences cell dynamics and orients cellular proliferation, aggregation, and differentiation, having an eventual impact on tissue regeneration [7,8]. Cells are able to feel the microenvironment and substrate texture on which they develop by changing their morphology, cytoskeleton configuration, intra- and extracellular signaling, and gene expression.

Therefore, increasing efforts are continuously being focused on advanced design and manufacturing technologies capable of generating and modifying the structures and surface topographies of biomaterials [9–11]. In most cases, material surface properties and topography are a consequence of its natural state. However, they can be also adjusted and controlled by means of machining processes, chemical etchings, and post-processing tools along the product development cycle. Several strategies for modifying material topographies and surface properties (towards hierarchical materials, structures, and multi-scale devices) have made use of conventional surface micromachining [12], laser ablation [13], micromolding [14], biomimetic templating [15], thin film deposition processes based on physical or chemical vapor deposition [16], sol–gel procedures [17], molecular self-assembly [18], and electro-spinning [19–21]. All these procedures require an expertise that is sometimes difficult to achieve and repeatability is not easy [22,23].

At present, relevant advances in computer-aided design and in high-precision additive manufacturing technologies are opening new horizons for the control of surface topography, even at a cellular level. Multi-scale and hierarchical structures with biomimetic features are achievable, even though conventional computer-aided design packages are only capable of handling Euclidean geometries and mainly rely on simple operations, thanks to the use of matrix-based programming for the incorporation of fractal details [24,25]. These advancements, together with the recent progress in additive manufacturing and rapid prototyping technologies, have enlarged the choice of materials capable of being additively conformed and allowed for a nanometric control of final geometries.

All this is relevant for materials and devices with advanced functionalities, in many cases the result of multi-scale approaches [26,27], although additional research linked to studying the impact of surface topography on cell behavior and fate are needed. The use of biomedical microdevices may prove useful for a more systematic, rapid and low-cost assessment of such impacts.

This work presents the complete development process and experimental validation of a biomedical microsystem for systematically studying the impact of surface topography on cell adhesion, motility, and overall behavior. The microsystem includes two pools, for culturing cells and for including chemical agents, nutrients, growth or trophic factors, and pathogens, among other possibilities. The pools are connected by several channels with different microtextures and it is expected the cells will crawl from one well to another along the different microtextured channels, as in fact they do in our experimental validation. Thus, the impact of channel surface topography on cell performance, as well as the influence of other relevant factors, can be assessed. The microtextures have been defined from the design stage and the microsystem has been manufactured using a combination of some of the more recent micromanufacturing technologies.

Previous pioneering research has also focused on the use of topographical features to control cell response and has clearly validated the impact on cell orientation, movement rates and cell activation, also putting forward the relevance of topographical control for the development of more adequate prostheses [28–32]. However, in most cases, the topographies are obtained by means of lithographic procedures and chemical attacks, which are difficult to control, require substantial experience, and typically lead to a set of probes with different textures. Consequently, the different probes are cultured independently and the number of experiments for analyzing the effects of surface topography on cell behavior is too high. Furthermore, more often than not, in studies focused on assessing the impact of surface topography on cell behavior by means of combining computer-aided design and rapid prototyping, the textures produced are based on combinations of simple geometries, based on conventional CAD operations using Euclidean geometries, which do not provide adequate representations of natural objects. Due to the complexity of natural materials [33], the use of such simple geometries does not provide biomimetic responses and therefore more recent procedures aimed at the incorporation of biomimetic fractal textures may be preferable [34].

In our opinion, the microsystem presented here is based on a novel approach, as the surface topographies can be precisely defined from the design stage and since it is a single microsystem it can include all the different topographies under study. Therefore, the proposed microsystem may

help optimize the use of resources and obtain important information for discussion, even with a few experiments, and also enable the assessment of the impact of different microtextures on cell behavior under identical experimental conditions.

Furthermore, the cell culture microsystem is aimed at the promotion of a real 3D cell culture environment in which the microchannels may help cells to crawl in the right direction for a systematic cost- and time-efficient study. In fact, recent studies have put forward that 1D cell culture resembles the real behavior of cells in three-dimensional environments rather than conventional 2D cell culture on dishes [35].

In our study, the combination of micro-channels with microtextured surfaces for orienting cell movement and for addressing the impact of surface topography on cell adhesion and motility is, to our knowledge, novel. In addition, the cell culture processes have been carried out by coating the surfaces with human mesenchymal stem cells (hMSCs) and conditioned medium (CM), obtained previously from the hMSCs culture supernatant as described earlier [36]. Recent reports have also put forward the extreme relevance of using adequate growth factors and related conditioned media obtained from the cells into tissue engineering scaffolds and cell culture platforms for promoting biological regulation, differentiation, proliferation, angiogenesis, and tissue viability [36–39].

The present work helps to validate their use in other kinds of biomedical microdevices aimed at studying cell dynamics and overall behavior. Results show outstanding values of cell adhesion and velocity and help to highlight the remarkable impact of surface topography on cell behavior, which can be rapidly studied with the proposed biodevice, which is validated for the first time. The following section summarizes the design and manufacturing procedures, the cell culture methods, and imaging techniques before presenting the main results and discussing them. The main conclusions and proposals for future studies and improvements are included towards the end of the study.

2. Experimental Section

2.1. Design Process

As mentioned in the introduction, the proposed system includes two microchambers at its lower end connected by several microchannels to guide cell movement, each with a different texture defined from the design stage. The cell motility experiment should begin to add cells (with or without growth factors or nutrients) to one of the chambers and, eventually, add growth factors, nutrients, chemicals, pathogens, *etc.* to the other one, so as to promote or prevent cell movement from one chamber to another. The design presented here is inspired by previous microsystems aimed at interacting with cells [40–42], although using better suited scales for interacting at the single-cell level without using ultra-high precision manipulators. In short, the overall structure, which mainly comprises the different walls of the two pools and the six microchannels, has been designed using conventional 3D computer-aided design methods. The CAD files can be converted into .stl format, currently the most common file type used in 3D additive manufacturing.

Different resources, such as digital light processing (DLP), laser stereolithography, selective laser sintering, or melting and fused deposition modeling, among others, can receive .stl files as information input. The specific method chosen would depend on the desired material and precision (in our case we used an EnvisionTEC digital light processing machine with acrylic resin for the master prototypes). The 3D design can also be converted into a black-white mask for mass-production of the overall structure using UV-lithographic approaches, more typical of the electronics industry. Subsequently, in order to incorporate the desired microtextures (capable of interacting at a cellular level) into the channels, additional design operations rely on the generation of fractal-based geometries via matrix-based approaches.

In such approaches, geometries are saved in the form of $[X, Y, Z(x, y)]$ matrices, X and Y being column vectors (with the x and y components of the working grid), and $Z(x, y)$ being a

column vector, whose components are the height values for each (x, y) couple. Fractal features can then be introduced to integrate controlled random textures into the regular meshes (z_0), as has been previously detailed [40]. In this paper we use fractional Brownian surface models [24,25] to incorporate the desired height fluctuations using the equation:

$$z(x, y) = z_0 + m \cdot \sum_{k=1}^{\infty} C_k \cdot \lambda^{-\alpha k} \cdot \sin(\lambda^k \cdot [x \cdot \cos(B_k) + y \cdot \sin(B_k) + A_k]) \quad (1)$$

The models use several random functions (A_k, B_k, C_k) and control constants (λ, α, m), and an initial height function “ z_0 ” can also be introduced. It is interesting to note that in fractional Brownian models [24,25], the fractal dimension “ D ” can be related to the exponent α , where $D = 3 - \alpha$, with $0 < \alpha < 1$. Consequently, higher values of “ α ” lead to more “planar” surfaces or textures and lower values of “ α ” lead to more “three-dimensional” ones, as detailed in Table 1 for the proposed microdevice. The “ λ ” parameter can be useful for changing surface roughness, while keeping fractal dimension constant, although in our case we have kept “ λ ” constant and only used “ α ” as a design parameter.

Consequently, in our case, roughness increases with the increase of fractal dimension, as can be seen from the data in Table 1. We have included roughness data according to some common definitions of roughness including R_a (arithmetic average of absolute values), R_{RMS} (root mean square) and R_t (maximum height of the profile). Recent significant research [32] has focused on the effects of surface roughness and fractal dimension on cell behavior and addressed them in a de-coupled manner with interesting results (also in agreement with most of our conclusions). However, in our case, we are just considering the possibility of controlling surface roughness and fractal dimension from the design stage and obtaining an experimentally validated microsystem that will hopefully be of value for studying the impact of surface microtexture on cell adhesion, dynamics and behavior. Additional details can be found elsewhere [24,25].

Figure 1a shows the computer-aided design of the complete microsystem, including the two square pools and 5 channels, designed using the fractal fractional Brownian surface model, with the following values of “ α ”: 0.1; 0.3; 0.5; 0.7 and 0.9 and with related fractal dimensions of: 2.9; 2.7; 2.5; 2.3 and 2.1. The microtextures obtained following this strategy are more similar to the irregular surfaces of biological materials than artificial textures based on pillars, struts, wood-pile structures, or similar designs based on Euclidean geometry. An additional planar control channel is included for the purpose of comparison, although in the present study we just concentrate on evaluating the textured channels.

The channels are 300 μm wide and around 7 mm long and the pools have a volume of $4 \times 2 \times 0.6 \text{ mm}^3$. The intermediate walls between channels are 300 μm wide and 200 μm high, which in some cases promotes cell escape from some channels, as discussed in the results section. We have used a grid for evaluating the aforementioned Brownian function with points separated 25 μm , according to the voxel size of the resin used for the additive manufacture of the master prototypes. As for the additional parameters, we have used $z_0 = 0$, $m = 1$ and $\lambda = 1.5$.

The dimensions of the microsystem have attempted to solve a compromise between manufacturing precision, manipulation facility and the potential for interacting at a single-cell level. We believe that the solution provided is interesting, versatile, and low-cost, as will be discussed towards the end of this paper.

2.2. Manufacturing Process

The master models or “green parts” are obtained by photopolymerization, using a digital light processing machine working on an additive or layer-by-layer approach. For that purpose, a Perfactory SXGA machine (EnvisionTec GmbH) has been used, together with the R11 EnvisionTec acrylate based photo-resin.

Figure 1b includes the initial prototypes (in orange resin) directly obtained by photo-polymerization from the three-dimensional geometries from the computer-aided design files. As the acrylic resin used for obtaining the master models is not apt for cell culture processes, replication technologies were used for producing final micro injected parts in poly(methyl methacrylate) (PMMA), as described further on.

Using the master model, a mold insert for micro injection molding was manufactured. In short, the process included gluing the masters to a thick copper substrate and using evaporation for coating the master and substrate with layers of 7 nm chromium and 50 nm gold. This was followed by immersion in a galvanic bath for nickel electroplating until a thickness of 6 mm was reached, followed by separation from the substrate and cutting and rinsing steps with ethyl acetate and acetone. This process led to a stiff homogeneous metal block that could endure the stresses from the injection molding process, shown in Figure 1c. Details can be found in prior reports [43].

The first action before starting the injection molding trials was to adjust the electroplated nickel mold inserts to a standard mold. Replication was accomplished on a Ferromatik Elektra 50S injection molding machine equipped with the necessary features, such as tool evacuation and vario-thermal-temperization. The latter means that the core of the molding tool was heated up prior to injecting the material. After filling, the tool core was cooled down for safe demolding without damaging the microstructured part. This procedure allowed for the replication of very fine structures with outstanding surface qualities. Figure 1c shows a replicated PMMA sample, together with the nickel mold insert. Micro injection molding stands out for the degree of precision attainable and for the possibility of manufacturing large series of replicas for systematic trials. In our case, 200 copies of the PMMA microsystem were obtained and at least 10 of them were used to adjust the cell-culture processes, as described in the following section.

The repeatability was outstanding and the final parts were compact, but without some of the typical injection molding problems, such as the presence of pores or wrapping, in spite of the precise dimensions of interest. The accuracy was remarkable, and even micrometric details, such as the presence of succinct longitudinal lines, resulting from the initial additive process and the separation between layers in the original acrylic prototypes or masters, could be perfectly replicated. The replicas obtained have several advantages when compared with the original acrylic rapid prototypes. They are made of bioinert polymers typically used in the medical industry (polycarbonate and poly(methyl methacrylate)), and are therefore adequate for *in vitro* trials. They are also transparent, which constitutes an enormous help for cell culture processes and related fluorescent microscopy tasks, while it is easier to manipulate them thanks to a supporting structure.

Regarding manufacturing precision, we would like to make some comments. It is important to highlight that, since the topographies are fractal and obtained by random processes, once the prototypes are manufactured it is complex to exactly find and visualize the same section in the design and in the final parts, which prevents quantitative roughness assessments. Trying with contact measurement procedures is not viable, as the measurement tip gets stuck to the surfaces due to the magnitude of the designed spikes and to the sudden changes of direction that the tip suffers. Most such contact measurement techniques are focused on the measurement of micro- (normally $< 5 \mu\text{m}$) and nano-features, and the magnitude of our artificially incorporated textures goes from 25 to 400 μm . As the additive manufacturing process used for the master prototypes had a layer depth of 25 μm and a movement precision of 25 μm , adequate structuring was based on using design features with sizes implying the use of at least 4–5 layers, so as to reach clearly visible features and to minimize the relative effect of the typical stepped geometries obtained in additive processes. Such dimensions and spiky textures prevent contact characterization and optical 3D tools are required.

However, based on our available data some additional interesting data on the precision of the whole process can be provided. For instance, a direct consequence of the precision of the additive manufacture machine is the obtaining of master prototypes, in which the last 25 micrometers of

the spiky textures are lost, thus leading to somewhat softer surfaces than those from the original CAD files.

For most applications of microtextured surfaces, such softer results may even be positive, as the devices will be a bit softer to the touch and more resistant, as fine needle-like details of 25 micrometers would anyway break down under the slightest mechanical request. In addition, after the optical measurements, the maximum profile heights of the different channels have been compiled in Table 1 for comparative assessment with the original values from the CAD files. The differences can be explained by considering not only the loss of the last portion of the spikes during additive manufacture, but also due to a valley depth decrease during metallization and injection, as possibly the material does not perfectly replicate the mold details.

In our opinion, the relevant result is linked to the possibility of controlling, from the design stage, the presence of different topographies on a single microsystem for cell culture. Our measurements show that the variations proposed in the design stage are present and the cell culture trials help to highlight the impact of the different microtextures on cell behavior; so, the main objective of the biodevice is achieved.

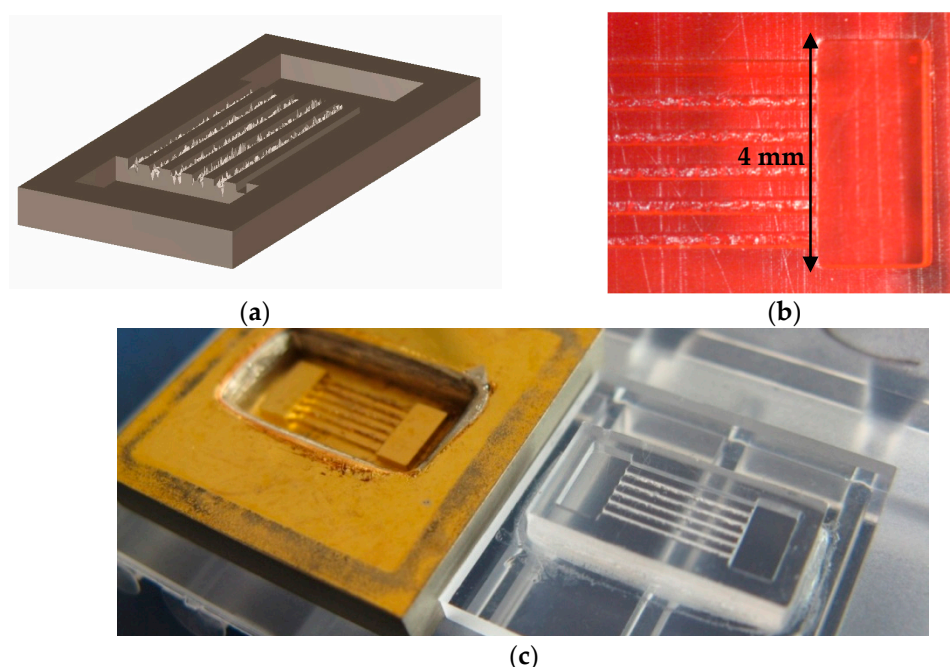


Figure 1. (a) Computer aided design of the multi-channel microsystem; (b) Master prototype obtained by additive manufacture (digital light projection or “DLP”); (c) Nickel mold insert and poly(methyl methacrylate) (PMMA) microsystem replica.

Table 1. Influence of parameter “ α ” on channel fractal dimension and roughness.

Channel number	1	2	3	4	5
Alpha (α)	0.9	0.7	0.5	0.3	0.1
Fractal dimension	2.1	2.3	2.5	2.7	2.9
Surface roughness (R_a), microns	24.3	27.8	33.2	37.8	40.9
Surface roughness (R_{rms}), microns	31.6	35.2	42.6	50.5	53.6
Surface roughness (R_t), microns	201.9	208.9	235.6	307.1	357.5
Surface roughness (R_t), microns (prototype)	135	160	185	220	255

2.3. Cell Culture Processes and Imaging Techniques

The hMSCs used here were isolated from human bone marrow samples from healthy anonymous donors provided by the hematology services of Hospital La Princesa, the Jiménez-Díaz Foundation, and the Biobank of the University of Málaga, and expanded as described previously [44,45] with the approval of the ethical committees of the institutions.

Cells were plated and incubated at 37 °C and 5% CO₂ using DMEM-LG 10% fetal bovine serum (FBS) from selected batches, and collected by treatment with 0.25% trypsin-EDTA. Cell culture mediums were prepared by the research services of the “Severo Ochoa” Molecular Biology Center (CSIC-UAM) as previously detailed [44,45] with some modifications. For the preparation of the hMSC conditioned medium, we used 8–10 p100 culture plates at 80% confluence for each batch, following previous successful experiences [36]. Cells were washed with PBS and incubated in DMEM-L starved of FBS and supplemented with 2 mM pyruvate for 24 h. Afterwards, the culture medium was collected and cleaned by centrifugation at 1500 rpm in a bench centrifuge for 5 min. The clean supernatant was cooled on ice for 30 min, centrifuged in a Sorvall machine to remove salt precipitations, and kept in 2 mL aliquots at –30 °C until use. We avoided any samples with repeated freeze-thaw. The process has been described previously [36].

To analyze the different microsystem replicas (PMMA) for cell adhesion and motility, materials were sterilized by placing them in a UV oven with a wavelength of 350 nm for 15 min and by thoroughly washing with phosphate buffer saline (PBS). For the adhesion studies, the microsystem replicas were pre-incubated with or without trophic factors (TFs) medium for 24–48 h previously, filled with cells, and left in culture for 24 h before verifying adhesion. For the motility studies, the microsystems were pre-incubated with or without TFs medium for 24–48 h previously, seeding the cells only in one of the pools, and subsequently left in culture for 24 h. The time was previously estimated so as to allow the cells to start crawling along the different channels towards the opposite pool.

The results from cell adhesion and motility on the microsystems were determined by staining with crystal violet. To this end, the cells were washed with PBS and fixed with formaldehyde 3.7% for 30 min, staining them with crystal violet at 0.5% for 30 min, washing the microsystems with water, and then allowing them to dry at room temperature. Representative images of the results were taken with an IX81 Olympus microscope linked to a DP72 digital camera controlled by cellD software. The main results are included and discussed in the following section. Before fixing, cell viability was studied by means of real time microscopy with the cells showing a healthy behavior with expanded cytoskeletons and clearly moving.

3. Results and Discussion

3.1. Impact of Surface Topography on Cell Adhesion

At first, hMSC showed almost no adhesion to the PMMA surface. However, the material offers excellent properties for tailoring microsystems that are useful in biotech applications. Therefore, we considered it of interest to coat the PMMA surface by a pre-treatment with TFs medium. Figure 2 presents the results of the adhesion study after having cultured the cells with TFs medium, on the PMMA multi-channel microsystem under study. In this case, for each channel, a total of five visual fields were photographed and used to reproduce the overall aspect of the cells (stained with crystal violet) adhered to the microsystem. The fractal dimension and roughness of the different channels appears to increase from left to right in Figure 2 with fractal dimension “*D*”, taking the values of 2.1, 2.3, 2.5, 2.7 and 2.9 (adimensional) for channels 1, 2, 3, 4 and 5 respectively. In order to quantify the influence of channel topography on cell adhesion, the cells per visual field were counted and the mean values with standard deviations are presented in Figure 3.

According to our results, an increase in surface roughness and fractal dimension promotes cell adhesion, with an almost linear tendency. The data represented in Figure 3 have been statistically

analyzed by carrying out a one-way ANOVA test to address the eventual significant influence of surface roughness and fractal dimension on cell adhesion. The null hypothesis stated “cell adhesion is similar in adjacent channels”, and we found several significant differences as detailed in Figure 3. An honest Tukey post-test was carried out to detect significant differences comparing the channels in couples. The analyses were carried out with confidence intervals of 95%. The data regarding significance of the ANOVA test are included in Table 2 and the results from the Tukey post-test, including *p*-values, are listed in Table 3. The influence of surface topography on cell adhesion is significant.

After application of the Tukey post-test to the data of the analysis of variance, two significantly different groups are found: one consisting of channels 1 and 2, with lower roughness, and one consisting of channels 3, 4, and 5, with higher roughness.

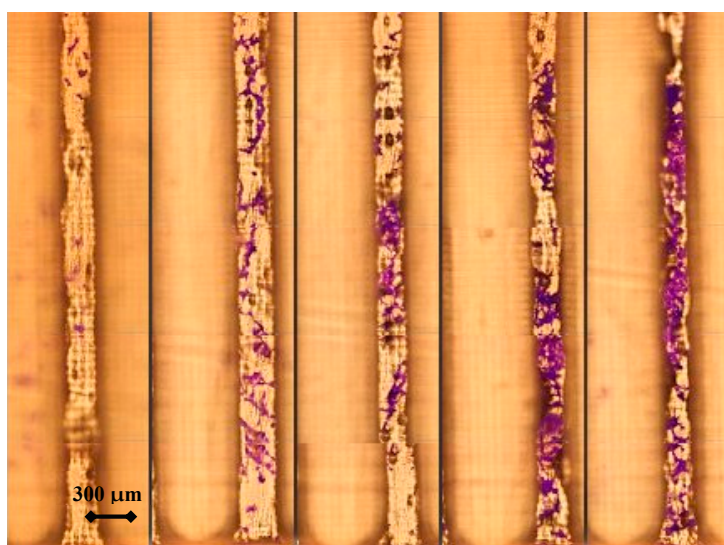


Figure 2. Results from the adhesion study of cells with growth factors cultured on the fractal microsystem: Cell distribution on the different channels showing the influence of channel geometry (microtexture) on cell adhesion. The roughness of the different channels increases from left to right.

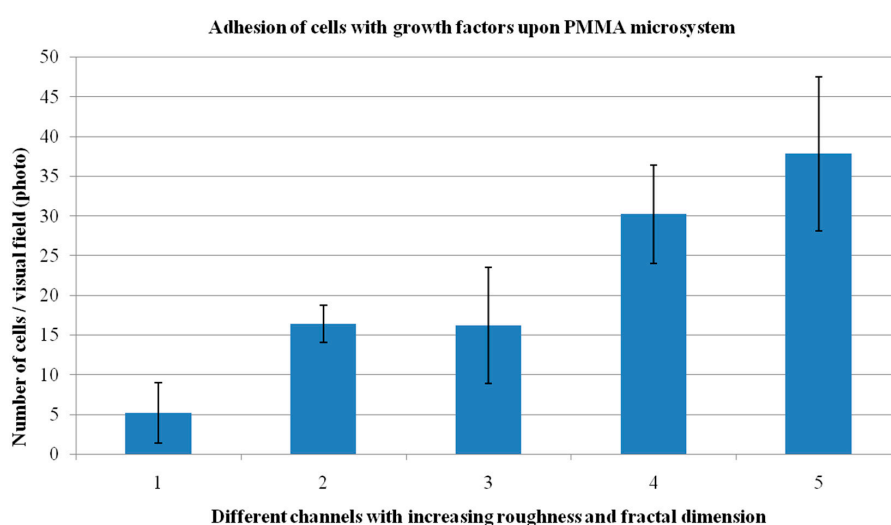


Figure 3. Results from the adhesion study of cells with TFs medium cultured on the fractal microsystem: Summary of the influence of channel topography on cell adhesion.

Table 2. Results from the ANOVA test. Estimates for the different channels with the expected upper and lower limits for adhered cells per visual field in each channel.

Channel	Mean	Std. error	95% Confidence interval	
1	5,200	2,868	782	11,182
2	16,400	2,868	10,418	22,382
3	16,200	2,868	10,218	22,182
4	30,200	2,868	24,218	36,182
5	37,800	2,868	31,818	43,782

Table 3. Tukey post-test: Two significantly different groups are found: one consisting of channels 1 and 2, with lower roughness, and one with the higher roughness, channels 3, 4, and 5. Based on observed means.

Tukey HSD		Mean difference (I-J)	Std. Error	Significant	95% Confidence interval	
(I) Chanel	(J) Chanel				Lower bound	Upper bound
1	2	−11.20	4.056	0.079	−23.34	0.94
	3	−11.00	4.056	0.087	−23.14	1.14
	4	−25.00 *	4.056	0.000	−37.14	−12.86
	5	−32.60 *	4.056	0.000	−44.74	−20.46
2	1	11.20	4.056	0.079	−0.94	23.34
	3	0.20	4.056	1.000	−11.94	12.34
	4	−13.80 *	4.056	0.021	−25.94	−1.66
	5	−21.40 *	4.056	0.000	−33.54	−9.26
3	1	11.00	4.056	0.087	−1.14	23.14
	2	−0.20	4.056	1.000	−12.34	11.94
	4	−14.00	4.056	0.019	−26.14	−1.86
	5	−21.60	4.056	0.000	−33.74	−9.46
4	1	25.00 *	4.056	0.000	12.86	37.14
	2	13.80 *	4.056	0.021	1.66	25.94
	3	14.00 *	4.056	0.019	1.86	36.14
	5	−7.60	4.056	0.362	−19.74	4.54
5	1	32.60 *	4.056	0.000	20.46	44.74
	2	21.40 *	4.056	0.000	9.26	33.54
	3	21.60 *	4.056	0.000	9.46	33.74
	4	7.60	4.056	0.362	−4.54	19.74

* The mean difference is significant at the 0.05 level.

These results can be taken into account for designing various biomedical microsystems and prostheses where cell adhesion should be promoted. It is interesting to note that surface roughness in the channels where the most relevant adhesion is obtained reaches values of around 40 microns for R_a , around 50 microns for RRMS and around 350 microns for R_t . Such values are at least an order of magnitude greater than the diameter of the cells cultured. Consequently, the channels can be considered as a real three-dimensional culture environment, in accordance with the fractal dimension values of the more adequate channels.

The result is in accordance with the adherent nature of mesenchymal stem cells; the increase in roughness and fractal dimension of the channels allows them to extend the number of their focal adhesion points with the surface, thereby helping them maintain their energy balance by themselves. The experiments carried out without the use of growth factors have not been included, as the number of cells per visual field was too low to obtain relevant conclusions (other than the importance of carrying out these studies with the use of such TFs medium).

3.2. Impact of Surface Topography on Cell Motility and Behavior

Figure 4 shows the results from the motility study after filling the origin well with cells and growth factors up to the entrance level of the different channels and after 24 h of subsequent

incubation. In this case, for each channel, a total of eleven visual fields were photographed and used to reproduce the overall aspect of the cells (stained with crystal violet) crawling on the microsystem. The whole length of the different channels can be seen from the origin pool, where the cells are cultured, to the end of each channel, just before meeting the final pool. It is important to note that the origin well is full with a network of viable cells and that the cells are able to enter all channels and crawl along them.

Again, the fractal dimension and roughness of the different channels appears to increase from left to right of the figure, with fractal dimension values of 2.1, 2.3, 2.5, 2.7, and 2.9 for channels 1, 2, 3, 4, and 5 respectively. Before summarizing and discussing the main results, we would like to highlight a couple of important and interesting tribological phenomena, which can be easily appreciated in the following Figures 5 and 6. Figure 5 shows a detailed view of the beginning portion of the three rougher channels (3, 4, and 5), from which several cells were even able to escape and tend to move towards their companion cells from other channels, as if they feel their presence and try to fill the inner space.

To avoid the effect, the separating walls between channels should have been made higher, as some peaks reaching values of around 100–120 μm (according to R_t) in these rougher channels, may have helped the cells to reach the upper part of the walls.

In any case, the behavior is quite interesting. We believe that cells may move into the channels possibly searching for higher oxygen concentrations than within the pool, where they are surrounded by several cells, and are attracted by the presence of an hMSC-CM coating on the channels.

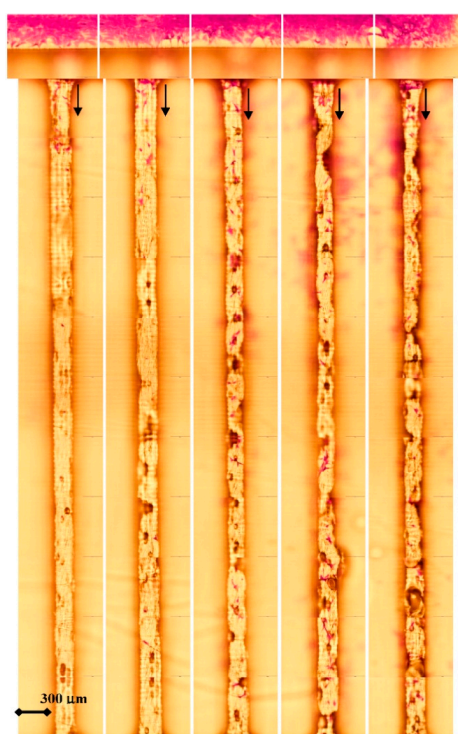


Figure 4. Results from the motility study of cells cultured on the fractal microsystem pre-treated with TFs medium: Origin well full of cells and cell distribution of cells along the channels. Fractal dimension and roughness increase from left to right.

The topography of the channels proves to be a key factor in their migration ability, as detailed in the following paragraphs. In addition, they seem to take into account the presence of companion cells from adjacent channels, with which they are connected in a kind of cellular circuit, and tend to communicate and migrate towards them. This phenomenon has been previously observed, where

hMSCs move into silicon columns of a silicon/porous silicon micro-patterning, communicating with their partners and migrating by the push forces applied from their companion cells located back in the center of the silicon hexagon [46].

Figure 6 helps put forward the relevance of using hMSC-CM as an aid for cell culture, especially when studying cell dynamics. Images 6a and 6b show a couple of detailed views of cells cultured on the pre-treated microsystem with the hMSC-CM, moving along channel 5, while images 6c and 6d show cells along the same channel but cultured on the surface without pre-treatment. It can be appreciated that the area without cells in the non-pre-treated microsystem is much larger than in pre-treated one.

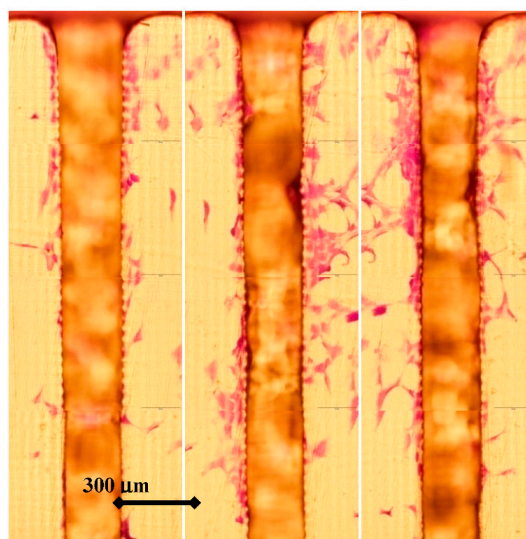


Figure 5. Detailed views of cells on the microsystem, escaping from the three rougher channels and migrating through their peripheries, after 24 h of motility study. The fractal dimension and roughness of the channels increases from left to right.

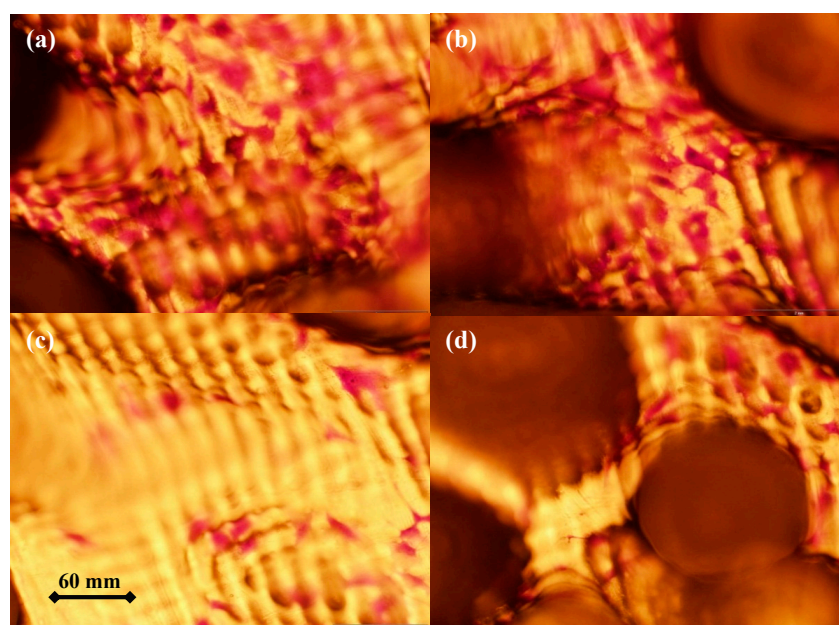


Figure 6. Detailed views of cells on the microsystem for highlighting the impact of hMSC-CM: (a,b) Cells cultured on pre-treatment surfaces; (c,d) Cells cultured on non-pre-treatment surfaces.

Thus, the entire results of the work are consistent with the utility of conditioned media, especially when generated by cells themselves, to functionalize biomaterial surfaces. In order to quantify the effect of surface topography on cell motility, we have directly counted the cells present inside the different channels, using the same visual fields that have helped us reproduce the whole microsystem, as shown in Figure 4. Each visual field (photograph) includes 600 μm of channel length and the cells can be easily perceived. As a summary, Figure 7 shows the distribution of cells along the different channels, taking into account the distance to the origin pool where the cells are cultured. In all channels, the zone near to the origin well is more populated with cells, showing that cells are able to enter all channels and start crawling along them. In channels 1, 2, and 3, the distribution of cells decreases with the distance to the origin pool. However, for the rougher channels, after an initial decrease in the number of cells with the distance to the origin pool, we can appreciate a relevant increase in cells in the most distant visual fields. Several cells in channels 4 and 5 almost reach the final pool.

Our interpretation is that the presence of an artificial surface roughness may promote opposing effects on the cells. On one hand, the mere presence of obstacles and artificial textures may be sensed by the cells as something that must be avoided to maintain their energy metabolism, as it may lead to stretched cytoskeleton configurations, or they may just be felt as strange and potentially harmful objects. On the other hand, the increase in the surface-to-volume ratio and adhesion with the roughness and the fractal dimension may provide additional anchorage options for cell pseudopodia and help them crawl. At lower roughnesses, the first effect seems to be prevalent, while at higher roughnesses the second effect stands out.

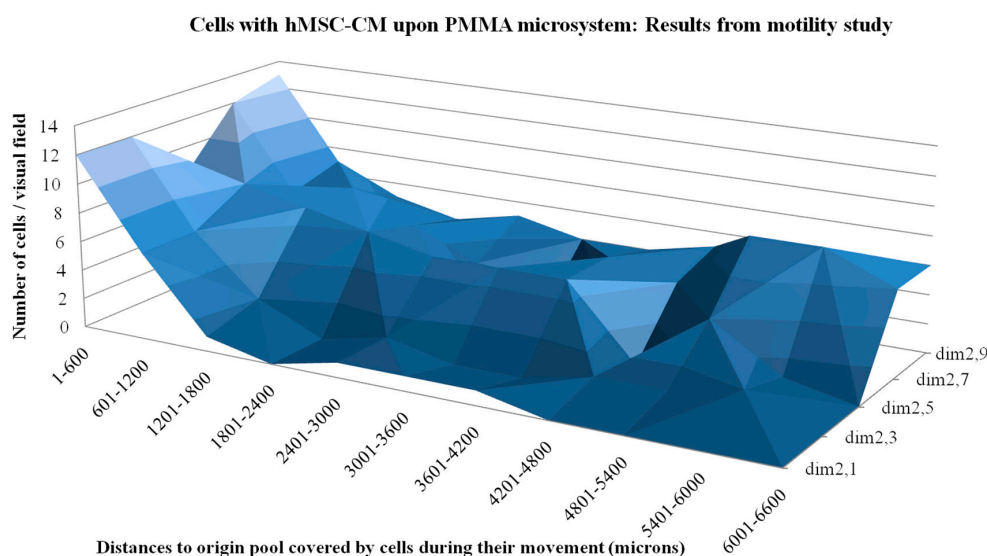


Figure 7. Results from the motility study of cells cultured on the fractal microsystem pre-incubated with hMSC-CM medium: Cell distance to origin well distribution along the different channels.

Taking into account that the cells have been cultured for 24 h in the motility study and that they have not reached the final pool, the proposed microsystem may also be useful for quantifying not only the impact of surface topography on cell adhesion, motility, and behavior, but also for obtaining an estimation of cell velocity on different surfaces. For such evaluation, in each channel, we located the positions of the ten most distant cells to the origin well and divided the distances covered by the culture time.

The mean values and related standard deviations are set out in Figure 8, which summarizes the influence of channel surface topography on cell velocity. A general increase in cell velocity with surface roughness and fractal dimension can be perceived, although if such values are too high, cell

velocity starts to decrease. We explain this phenomenon by taking into account that an increase of adhesion probably provides additional anchorage options for the pseudopodia, although too much 3D topography, roughness, and fractal dimension prevent cell migration through the channels, and may enable them to escape from the channels.

The data represented in Figure 8 have been statistically analyzed, again using an ANOVA study and a Tukey post-test for paired comparisons. As the null hypothesis stated: “cell velocity is similar in adjacent channels”. The data regarding significance of the ANOVA test are included in Table 4 and the results from the Tukey post-test, including *p*-values, are listed in Table 5. According to the analysis of variance, the influence of surface topography on cell speed is significant. After application of the Tukey post-test to the analysis of variance data, two significantly different groups are again found, one consisting of channels 1 and 2, with lower roughness, and one consisting of channels 3, 4, and 5, with higher roughness.

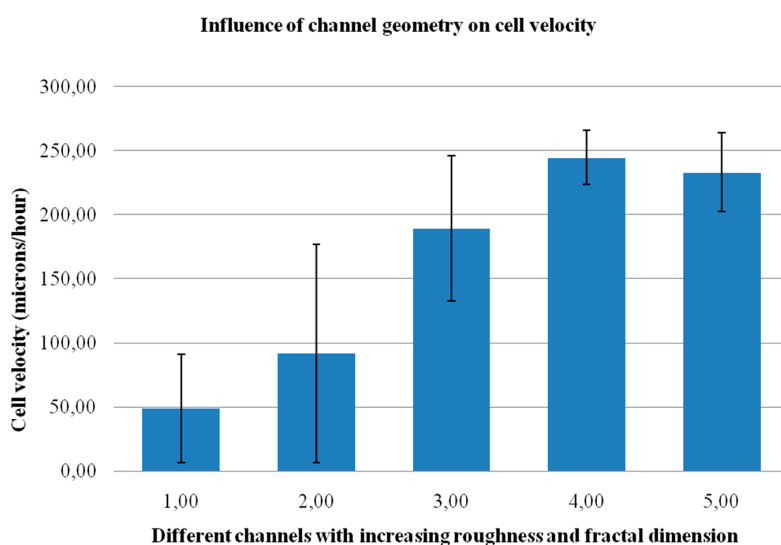


Figure 8. Results from the motility study of cells cultured on the fractal microsystem pre-incubated with TFs medium: Summary of the influence of channel geometry (microtexture) on cell velocity.

Table 4. Results from the ANOVA test. Estimates for the different channels with the expected upper and lower limits for cell speed in each channel.

Channel	Mean	Std. Error	95% Confidence Interval	
1	19,600	6,610	6,286	32,914
2	36,667	6,610	23,353	49,981
3	75,733	6,610	62,419	89,047
4	97,800	6,610	84,486	111,114
5	93,200	6,610	79,886	106,514

The results are in accordance with the behavior of hMSCs. Mesodermal stem cells isolated from bone marrow have an adherent nature and are able to respond to their adhesion surface, such as roughness and fractal dimension, in our case. The combination of the PMMA microsystem and its pre-treatment with TFs medium constitutes a valid system to evaluate the effect of different compounds, such as chemical agents, drugs, viruses, or toxins in hMSCs adhesion behavior. This is important due to the regenerative properties against trauma or aging carried out *in vivo* by these cells. In the microsystem, hMSCs reach a velocity value of 6000 $\mu\text{m}/\text{day}$, helping to show the positive impact of incorporating design-defined fractal microtextures to promote cell motility and eventual tissue growth. Results from 2D cell cultures on planar substrates have previously led to values of 700 $\mu\text{m}/\text{day}$, while the use of micro-patterned grooves has promoted a velocity of up to

1000 $\mu\text{m}/\text{day}$ and encouraged interest in using surface patterns to promote cell culture strategies [47]. Recent research has also demonstrated the beneficial use of anisotropic nanopatterns to drive stem cell migration and has shown cell velocity values of up to 960 $\mu\text{m}/\text{day}$ along the direction parallel to the pattern and up to 600 $\mu\text{m}/\text{day}$ along the direction perpendicular to the pattern [48].

In our opinion, the use of design-defined microtextured channels provides a more three-dimensional approach, in accordance with recent results, highlighting that 1D cell culture is more similar to 3D conditions than more conventional 2D cell culture on planar surfaces [35]. According to Doyle and colleagues, cell migration in both 1D and 3D is rapid, uniaxial, and independent of extra-cellular matrix ligand density, in contrast to 2D cultures, which brings out the need for alternative solutions aimed at a more adequate reproduction of the 3D environment [48]. We truly believe that our approach of providing 1D cell culture along channels with inner three-dimensional features can help with further studies linked to comparing 1D, 2D, and 3D cell culture, as well as take into account non-integer values, using a fractal-based definition of dimension. The noteworthy values of cell velocity obtained help to verify the potential of these kinds of design combinations and of the relevant use of a pre-treatment with TFs medium.

Table 5. Tukey post-test: Two significantly different groups are found, one consisting of channels 1 and 2, with lower roughness, and one with higher roughness, channels 3, 4, and 5.

Tukey HSD		Mean Difference (I-J)	Std. Error	Significant	95% Confidence Interval	
(I) Chanel	(J) Chanel				Lower Bound	Upper Bound
1	2	-17.0667	9.34861	0.372	-43.6303	9.4969
	3	-56.1333 *	9.34861	0.000	-82.6969	-29.5697
	4	-78.2000 *	9.34861	0.000	-104.7636	-51.6364
	5	-73.6000 *	9.34861	0.000	-100.1636	-47.0364
2	1	17.0667	9.34861	0.372	-9.4969	43.6303
	3	-39.0667 *	9.34861	0.001	-65.6303	-12.5031
	4	-61.1333 *	9.34861	0.000	-87.6969	-34.5697
	5	-56.5333 *	9.34861	0.000	-83.0969	-29.9697
3	1	56.1333 *	9.34861	0.000	29.5697	82.6969
	2	39.0667 *	9.34861	0.001	12.5031	65.6303
	4	-22.0667	9.34861	0.145	-48.6303	4.4969
	5	-17.4667	9.34861	0.349	-44.0303	9.0969
4	1	78.2000 *	9.34861	0.000	51.6364	104.7636
	2	61.1333 *	9.34861	0.000	34.5697	87.6969
	3	22.0667	9.34861	0.145	-4.4969	48.6303
	5	4.6000	9.34861	0.988	-21.9636	31.1636
5	1	73.6000 *	9.34861	0.000	47.0364	100.1636
	2	56.5333 *	9.34861	0.000	29.9697	83.0969
	3	17.4667	9.34861	0.349	9.0969	44.0303
	4	-4.6000	9.34861	0.988	-31.1636	21.9636

* The mean difference is significant at the 0.05 level.

As for the future, we expect to carry out additional experiments with the microsystem replicas for specifically focusing on these interesting behaviors, which may also be influenced by the type of cell cultures, the incorporation of additional chemicals, the use of special surface functionalizations, and the total number of cells cultured. In any case, we truly believe that the presented microsystem is an interesting resource for further studying cell dynamics and behavior, as the results presented show. Another interesting issue is that if cells are cultured for longer times, this is linked to studying the influence of surface topography on the differentiation of cells into relevant tissues and final tissue viability. In future trials, we expect to evaluate which channels are more adipogenic and which more osteogenic, according to groundbreaking research [49].

The use of ultrahigh precision additive manufacturing technologies, especially direct laser writing based on two-photon polymerization [50,51], may help to further reduce the size of the

proposed microsystem down to 10 μm -wide channels and surface roughness of around 1–5 μm , as we have already verified [42]. Such size reduction may help with trying to obtain a single row of cells crawling along the channels to obtain a more ideal single cell behavior and to assess the effect of more subtle topographies on cell response. However, such size reduction entails considerable manipulation difficulties and novel challenges linked to cell culture, as well as some yet unsolved limitations regarding mass production.

Combining manufacturing technologies in order to obtain similar microsystems to the one proposed here but covering a wider range of surface topographies, from hundreds of nm to hundreds of μm , will be useful for increasing our knowledge of cell dynamics and response to surface topography. We expect to achieve this in forthcoming studies in collaboration with all colleagues that may find this approach of interest or, at least, of help as a complement to their current methods. Fractal-based design approaches, together with additive manufacture and replication techniques, may well indeed be useful for controlling such textures from the design stage. Additional research will be devoted to applying the proposed textures to the surfaces of more complex biodevices, as the use of biomimetic textures has been reported as a key towards more effective medical devices [52].

4. Main Conclusions

In this study we have presented the complete development and experimental validation of a microsystem aimed to systematically assess the impact of surface topography on cell adhesion, behavior, and dynamics. The microsystem includes two pools: for culturing cells, and for including chemical agents, nutrients, growth or trophic factors, and pathogens, among other interesting possibilities. The pools are connected by several channels with different microtextures, along which cells are able to crawl from one well to another. The impact of channel surface topography on cell performance, as well as the influence of other relevant factors, can therefore be assessed. The microsystem stands out for its ability to precisely define the surface topographies from the design stage and also has the advantage of including the different textures of study in a single device. The cell culture processes carried out, using human mesenchymal stem cells (hMSCs) with the incorporation of growth factors, have helped validate the microsystem performance and bring to light interesting phenomena and behaviors of cells. The impact of surface topography on cell adhesion, motility, and velocity has been quantified, and the relevance of using growth factors for these kinds of studies has been analyzed. The main results are in line with the experiences of several colleagues, but quite a few interesting questions, which will guide future studies, have also arisen.

Acknowledgements: This work was carried out with the support of the European Community. We appreciate the support of the European Research Infrastructure EUMINAfab (funded under the FP7 specific programme Capacities, Grant Agreement Number 226460) and its partner the Karlsruhe Institute of Technology. We are also grateful to Dieter Maas and to Thomas Schaller for their kind help and support for the EUMINAfab 1099 proposal on “Replication of advanced scaffolds with biomimetic fractal features”. This work was partly carried out with the support of the Karlsruhe Nano Micro Facility (KNMF, www.knmf.kit.edu), the Helmholtz Research Infrastructure at Karlsruhe Institute of Technology.

We acknowledge Jürgen Stampfl, Head of the Additive Manufacturing Laboratory at the Technical University of Vienna, for the access to the digital light processing machine and for his support for obtaining the initial master models. We acknowledge Jesús Juan Ruíz, Head of the Statistics Teaching Unit at the School of Industrial Engineering, TU Madrid, (www.etsii.upm.es/ingor/estadistica/), for his kind and detailed support with the statistical analyses and with understanding the secrets of the multiple comparisons and of the Tukey post-test. We acknowledge reviewers for their proposals for improvement, which have helped us to achieve a much more detailed final version. Their selection of interesting references also made us aware of interesting alternatives to the processes used here.

Author Contributions: All authors took part in the definition of the microsystem concept, research procedure and experimental design. Andres Diaz Lantada carried out computer-aided design and manufacture of the biomedical micro-system. Hernán Alarcón Iniesta and Josefa Predestinación García-Ruíz performed the *in vitro* assessment by means of cell culture trials. Discussion of results and analyses linked to future challenges were performed by all authors.

Conflicts of Interest: The authors declare no conflict of interest.

References

1. Archard, J. Surface topography and tribology. *Tribology* **1974**, *7*, 213–220. [[CrossRef](#)]
2. Bushan, B.; Israelachvili, J.; Landman, U. Nanotribology: Friction, wear and lubrication at the atomic scale. *Nature* **1995**, *374*, 607–616. [[CrossRef](#)]
3. Barthlott, W.; Neinhuis, C. Purity of the sacred lotus, or escape from contamination in biological surfaces. *Planta* **1997**, *202*, 1–8. [[CrossRef](#)]
4. Buxboim, A.; Discher, D.E. Stem cells feel the difference. *Nat. Methods* **2010**, *7*, 695–697. [[CrossRef](#)] [[PubMed](#)]
5. Berginski, M.; Hüpkes, J.; Schulte, M.; Schöpe, G.; Stiebig, H.; Rech, B. The effect of front ZnO:Al surface texture and optical transparency on efficient light trapping in silicon thin-film solar cells. *J. Appl. Phys.* **2007**. [[CrossRef](#)]
6. Briones, V.; Aguilera, J.M.; Brown, C. The effect of surface topography on color and gloss of chocolate samples. *J. Food Eng.* **2006**, *77*, 776–783. [[CrossRef](#)]
7. Francesco, G.; Tirinato, L.; Battista, E.; Causa, F.; Liberale, C.; di Fabrizio, E.M.; Decuzzi, P. Cells preferentially grow on rough substrates. *Biomaterials* **2010**, *31*, 7205–7212.
8. Kumar, G.; Waters, M.S.; Farooque, T.M.; Young, M.F.; Simon, C.G., Jr. Freeform fabricated scaffolds with roughened struts that enhance both stem cell proliferation and differentiation by controlling cell shape. *Biomaterials* **2012**, *33*, 4022–4030. [[CrossRef](#)] [[PubMed](#)]
9. Thomas, W.E.; Discher, D.E.; Shastri, V.P. Mechanical regulation of cells by materials and tissues. *MRS Bull.* **2010**, *35*, 578–583. [[CrossRef](#)]
10. Chen, W.L.; Likhitanichkul, M.; Ho, A.; Simmons, C.A. Integration of statistical modeling and high-content microscopy to systematically investigate cell-substrate interactions. *Biomaterials* **2010**, *31*, 2489–2497. [[CrossRef](#)] [[PubMed](#)]
11. Buxboim, A.; Rajalgopal, K.; Brown, A.E.; Discher, D.E. How deeply cells feel: Methods for thin gels. *J. Phys. Condens. Matter.* **2010**. [[CrossRef](#)] [[PubMed](#)]
12. Madou, M.J. *Fundamentals of Microfabrication: The Science of Miniaturization*, 2nd ed.; CRC Press: New York, NY, USA, 2002.
13. Chandra, P.; Lai, K.; Sunj, H.J.; Murthy, N.S.; Kohn, J. UV laser-ablated surface textures as potential regulator of cellular response. *Biointerphases* **2010**, *5*, 53–59. [[CrossRef](#)] [[PubMed](#)]
14. Martin, C.R.; Aksay, I.A. Microchannel molding: A soft lithography-inspired approach to micrometer-scale patterning. *J. Mater. Res.* **2005**, *20*, 1995–2003. [[CrossRef](#)]
15. Pulsifier, D.P.; Lakhtakia, A. Background and survey of bioreplication techniques. *Bioinspir. Biomim.* **2011**. [[CrossRef](#)] [[PubMed](#)]
16. Kwasny, W. Predicting properties of PVD and CVD coatings based on fractal quantities describing their surface. *J. Achiev. Mater. Manuf. Eng.* **2009**, *37*, 125–192.
17. Jedlicka, S.S.; McKenzie, J.L.; Leavesley, S.L.; Little, K.M.; Webster, T.J.; Robinson, J.P.; Nivens, D.E.; Rickus, J.L. Sol-gel derived materials as substrates for neuronal differentiation: Effects of surface features and protein conformation. *J. Mater. Chem.* **2007**, *16*, 3221–3230. [[CrossRef](#)]
18. Rahmawan, Y.; Xu, L.; Yang, S. Self-assembly of nanostructures towards transparent, superhydrophobic surfaces. *J. Mater. Chem. A* **2013**, *1*, 2955–2969. [[CrossRef](#)]
19. Centola, M.; Rainer, A.; Spadaccio, C.; de Porcellinis, S.; Genovese, J.A.; Trombetta, M. Combining electrospinning and fused deposition modeling for the fabrication of a hybrid vascular graft. *Biofabrication* **2010**. [[CrossRef](#)] [[PubMed](#)]
20. Ballester-Beltran, J.; Lebourg, M.; Capella, H.; Diaz Lantada, A.; Salmerón-Sánchez, M. Robust fabrication of electrospun-like polymer mats to direct cell behaviour. *Biofabrication* **2014**. [[CrossRef](#)] [[PubMed](#)]
21. Rogers, C.M.; Morris, G.E.; Gould, T.W.A.; Ball, R.; Toumpaniari, S.; Harrington, H.; Dixon, J.E.; Shakesheff, K.M.; Segal, J.; Rose, F.R. A novel technique for the production of electrospun scaffolds with tailored 3D micro-patterns using additive manufacturing. *Biofabrication* **2014**. [[CrossRef](#)] [[PubMed](#)]
22. Gad-el-Hak, M. *The MEMS Handbook*; CRC Press: New York, NY, USA, 2003.
23. Naik, V.M.; Mukherjee, R.; Majumder, A.; Sharma, A. Super functional materials: Creation and control of wettability, adhesion and optical effects by meso-texturing of surfaces. *Curr. Trends Sci. Platin. Jubil. Spec.* **2009**, 129–148.

24. Mandelbrot, B. *The Fractal Geometry of Nature*; W.H. Freeman & Co. Ltd.: San Francisco, CA, USA, 1982.
25. Falconer, K. *Fractal Geometry: Mathematical Foundations and Applications*; John Wiley & Sons Ltd.: West Sussex, UK, 2003.
26. Bückmann, T.; Stenger, N.; Kadic, M.; Kaschke, J.; Frölich, A.; Kennerknecht, T.; Eberl, C.; Thiel, M.; Wegener, M. Tailored 3D mechanical metamaterials made by dip-in direct-laser-writing optical lithography. *Adv. Mater.* **2012**, *24*, 2710–2714. [[CrossRef](#)] [[PubMed](#)]
27. Röhrig, M.; Thiel, M.; Worgull, M.; Hölscher, H. Hierarchical structures: 3D direct laser writing of nano-microstructured hierarchical gecko-mimicking surface. *Small* **2012**, *8*, 3009–3015. [[CrossRef](#)] [[PubMed](#)]
28. Clark, P.; Connolly, P.; Curtis, A.S.G.; Dow, J.A.T.; Wilkinson, C.D.W. Topographic control of cell behavior. *Development* **1987**, *9*, 439–448.
29. Curtis, A.S.G.; Wilkinson, C.D.W. Topographical control of cells. *Biomaterials* **1997**, *18*, 1573–1583. [[CrossRef](#)]
30. Flemming, R.G.; Murphy, C.J.; Abrams, G.A.; Goodman, S.L.; Nealey, P.F. Effects of synthetic micro- and nano-structured surfaces on cell behavior. *Biomaterials* **1999**, *20*, 573–588. [[CrossRef](#)]
31. Crouch, A.S.; Miller, D.; Luebke, K.J.; Hu, W. Correlation of anisotropic cell behaviors with topographic aspect ratio. *Biomaterials* **2009**, *30*, 1560–1567. [[CrossRef](#)] [[PubMed](#)]
32. Gentile, F.; Medda, R.; Cheng, L.; Battista, E.; Scopelliti, P.E.; Milani, P.; Cavalcanti-Adam, E.A.; Decuzzi, P. Selective modulation of cell response on engineered fractal silicon substrates. *Sci. Rep.* **2013**, *3*, 1461. [[CrossRef](#)] [[PubMed](#)]
33. Place, E.S.; Evans, N.; Stevens, M. Complexity in biomaterials for tissue engineering. *Nat. Mater.* **2009**, *8*, 457–469. [[CrossRef](#)] [[PubMed](#)]
34. Díaz Lantada, A.; Pareja Sánchez, B.; Gómez Murillo, C.; Urbieto Sotillo, J. Fractals in tissue engineering: Toward biomimetic cell-culture matrices, microsystems and microstructured implants. *Expert Rev. Med. Devices* **2013**, *10*, 629–648. [[CrossRef](#)] [[PubMed](#)]
35. Doyle, A.D.; Wang, F.W.; Matsumoto, K.; Yamada, K. One-dimensional topography underlies three-dimensional fibrillar cell migration. *J. Cell Biol.* **2009**, *184*, 481–490. [[CrossRef](#)] [[PubMed](#)]
36. Díaz Lantada, A.; Alarcón Iniesta, H.; Pareja Sánchez, B.; García-Ruiz, J.P. Free-form rapid-prototyped PDMS scaffolds incorporating growth factors promote chondrogenesis. *Adv. Mater. Sci. Eng.* **2014**. [[CrossRef](#)]
37. Richardson, T.P.; Peters, M.C.; Ennett, A.B.; Mooney, D.J. Polymeric system for dual growth factor delivery. *Nat. Biotechnol.* **2001**, *19*, 1029. [[CrossRef](#)] [[PubMed](#)]
38. Perets, A.; Baruch, Y.; Weisbuch, F.; Shoshany, G.; Neufeld, V.; Cohen, S. Enhancing the vascularization of three-dimensional porous alginate scaffolds by incorporating controlled release basic fibroblast growth factor microspheres. *J. Biomed. Mater. Res. A* **2003**, *65*, 489–497. [[CrossRef](#)] [[PubMed](#)]
39. Laschke, M.W.; Rücker, M.; Jensen, G.; Carvalho, C.; Mülhaupt, R.; Gellrich, N.C.; Menger, M.D. Incorporation of growth factor containing Matrigel promotes vascularization of porous PLGA scaffolds. *J. Biomed. Mater. Res. A* **2008**, *85*, 397–407. [[CrossRef](#)] [[PubMed](#)]
40. Díaz Lantada, A. *Handbook on Advanced Design and Manufacturing Technologies for Biomedical Devices*; Springer: New York, NY, USA, 2013.
41. Díaz Lantada, A.; Endrino, J.L.; Mosquera, A.A.; Lafont, P. Design and rapid prototyping of DLC coated fractal surfaces for tissue engineering applications. *J. Phys. Conf. Ser.* **2010**. [[CrossRef](#)]
42. Hengsbach, S.; Díaz Lantada, A. Rapid prototyping of multi-scale biomedical microdevices by combining additive manufacturing technologies. *Biomed. Microdevices* **2014**, *16*, 617–627. [[CrossRef](#)] [[PubMed](#)]
43. Díaz Lantada, A.; Piotter, V.; Plewa, K.; Barié, N.; Guttmann, M.; Wissmann, M. Towards mass production of microtextured microdevices: Linking rapid prototyping with micro injection molding. *Int. J. Adv. Manuf. Technol.* **2014**. [[CrossRef](#)]
44. Lennon, D.P.; Haynesworth, S.E.; Bruder, S.P.; Jaiswal, N.; Caplan, A.I. Human and animal mesenchymal progenitor cells from bone marrow: Identification of serum for optimal selection and proliferation. *In vitro Cell. Dev. Biol.* **2006**, *32*, 602–611. [[CrossRef](#)]
45. Ogueta, S.; Muñoz, J.; Obregon, E.; Delgado-Baeza, E.; García-Ruiz, J.P. Prolactin is a component of the human synovial liquid and modulates the growth and chondrogenic differentiation of bone marrow-derived mesenchymal stem cells. *Mol. Cell. Endocrinol.* **2002**, *190*, 51–63. [[CrossRef](#)]

46. Ynsa, M.D.; Dang, Z.Y.; Manso-Silvan, M.; Song, J.; Azimi, S.; Wu, J.F.; Liang, H.D.; Torres-Costa, V.; Punzon-Quijorna, E.; Breese, M.B.; *et al.* Reprogramming hMSCs morphology with silicon/porous silicon geometric micro-patterns. *Biomed. Microdevices* **2014**, *16*, 229–236. [[CrossRef](#)] [[PubMed](#)]
47. Hoffmann, M.; Kuska, J.-P.; Zscharnack, M.; Loeffler, M.; Galle, J. Spatial organization of mesenchymal stem cells *in vitro*—Results from a new individual cell-based model with podia. *PLoS ONE* **2011**, *6*, 1–15. [[CrossRef](#)] [[PubMed](#)]
48. Jachetti, E.; di Renzo, C.; Meucci, S.; Nocchi, F.; Beltram, F.; Cecchini, M. Wharton’s jelly human mesenchymal stem cell contact guidance by noisy nanotopographies. *Nat. Sci. Rep.* **2014**, *4*, 1–9. [[CrossRef](#)] [[PubMed](#)]
49. Yao, X.; Peng, R.; Ding, J. Cell-material interactions revealed via material techniques of surface patterning. *Adv. Mater. Mater. Views* **2013**, *25*, 5257–5286. [[CrossRef](#)] [[PubMed](#)]
50. Ostendorf, A.; Chichkov, B.N. Two-photon polymerization: A new approach to micromachining. *Photon. Spectra* **2006**, *40*, 72–80.
51. Hermatsweiler, M. 3D-druck erobert die mikroskala. *Laser Tech. J.* **2013**, *10*, 55–57. [[CrossRef](#)]
52. Longoni, S.; Sartori, M. Fractal geometry of nature (bone) may inspire medical devices shape. *Nat. Prec.* **2010**, *1*, 1–16.



© 2015 by the authors; licensee MDPI, Basel, Switzerland. This article is an open access article distributed under the terms and conditions of the Creative Commons by Attribution (CC-BY) license (<http://creativecommons.org/licenses/by/4.0/>).